

COMPARISON OF PEDIATRIC AND YOUNG ADULT FAR-SIDE HEAD KINEMATICS IN LOW-SPEED LATERAL AND OBLIQUE IMPACTS

Emily A. Mathews

Sriram Balasubramanian

Drexel University

United States of America

Thomas Seacrist

Matthew R. Maltese

Kristy B. Arbogast

Children's Hospital of Philadelphia

United States of America

Richard W. Kent

Jason Forman

University of Virginia, Center for Applied Biomechanics

United States of America

Kazuo Higuchi

Hiromasa Tanji

Takata Corporation

Japan

Paper Number 13-0345

ABSTRACT

The importance of head injuries to restrained far seat occupants has been previously documented. Control of the kinematics leading to these injuries can likely be achieved by improved torso lateral restraint. In adults, seat belt pre-tensioning reduced lateral head displacement by approximately 200 mm in far-side impacts. Children, however, may demonstrate greater lateral movement as previous studies have shown greater spine flexibility in the pediatric population relative to adults. The objective of this study was to investigate pediatric and young adult far-side head kinematics in low-speed lateral and oblique impacts and explore the effect of pre-tensioning.

Thirty male human volunteers, ages 9-14 years (n=20) and 18-30 years (n=10), were tested on a low-speed, sub-injurious crash sled at either 60° or 90°. The safety envelope of the crash pulse was defined by an amusement park bumper car impact. The acceleration pulse was provided by a custom-designed hydro-pneumatically-driven sled system composed of a cart on a set of low friction rails (max pulse: 1.91 g; rise time: 53.8 ms; pulse duration: 146.5 ms). Each subject was restrained by a custom-fit automotive three-point belt system with an electromechanical motorized seat belt retractor (EMSR). The EMSR activated 200 ms prior to initiation of the crash pulse and provided a pre-tensioning load of approximately 300N, with a rise time to peak load of 100 ms. The restraint system was designed such that the EMSR could be active or

inactive. Photo-reflective targets were attached to a tight-fitting head piece on each subject and adhered to skeletal landmarks on the spine, shoulders, sternum, and legs as well as along the shoulder belt. A 3-D near-infrared target tracking system quantified the position of the targets throughout the event. Subjects participated in a set of 8 randomized trials, four with EMSR activation and four without EMSR activation. Maximum head and spine excursions were measured.

EMSR activation significantly reduced the magnitude of head and spine kinematics. With EMSR activation, lateral head excursion decreased by an average of 96 mm and 114 mm, and T1 excursions were reduced by an average of 105 mm and 106 mm for oblique and lateral impacts, respectively.

Although EMSR activation to reduce seat belt slack is primarily indicated as a frontal impact countermeasure, these data demonstrate its efficacy in reducing head excursion in far-side impacts. Low-speed human volunteer tests provide insight into occupant motion at these impact angles in the presence of active musculature. These results are useful for the development of rear seat countermeasures.

INTRODUCTION

Far-side occupants are at a substantial risk of severe injury and death in crashes. They are involved in 30% of side impact injuries and account for 40% of

all occupants (Digges and Dalmotas 2001). In a far-side crash, the head is the most commonly injured region for both belted and unbelted occupants (Digges et al. 2005). Contact patterns of far side occupants indicate that current restraint systems are not optimally effective in keeping far-side occupants from striking structures on the opposite side of the vehicle or other occupants (Ryb et al. 2009). Most of the current far-side literature focuses on the front seat adult occupant (Digges and Dalmotas 2001; Parenteau 2006a; Parenteau 2006b; Viano and Parenteau 2010; Douglas et al. 2011). Little attention has been given to the rear seat occupant in far-side crashes. Maltese et al. (2005) investigated injury patterns of restrained far-side pediatric occupants and found the head to be the most frequently injured region.

The prevalence of head injury in far-side occupants suggests that the occupant's torso slips out of the shoulder belt such that the torso is no longer restrained, allowing for greater head displacement (Mackay et al. 1991; Stolinski et al. 1998a; Douglas et al. 2011). Studies have described the nature of the torso-belt interaction for adult occupants in far-side impacts by using post-mortem human subjects (PMHS), anthropomorphic test devices (ATD), and human volunteers. Horsch (1980) described the effect of impact angle on belt retention with an ATD. He concluded that for far-side impacts, the belt remained contact with the torso for impact angles less than 45°, and that the torso rolled out of the shoulder belt for impact angles between 60° and 90° (from full frontal). The author also stated that in the instances where the torso escaped the shoulder belt, most of the torso's kinetic energy had dissipated, resulting in little motion outside of the belt. Bidez et al. (2005) found that the Hybrid III 6 year old and Hybrid III 5th female (as surrogate for 50th percentile 12 year old) experience torso rollout when restrained by a standard 3-pt belt system and subjected to a far-side impact.

Belt interaction with the torso and the clavicle has been identified as a particular challenge in biofidelity for the ATD and as a result, the magnitude of excursion seen in human surrogates is likely even more (Törnvall et al. 2005; Pintar et al. 2006; Douglas et al. 2007). Simulated lateral sled tests conducted by Horsch et al. (1979) with PMHS showed that when the shoulder belt anchor was opposite the side of the impact, the PMHS rotated out of the shoulder belt onto the adjacent seat. Torso-rollout has been confirmed in PMHS far-side sled tests (8.3g) at both 60° and 90° (Douglas et al. 2007). Douglas et al. also tested adult human volunteers in a

test rig that rotated laterally by 90° providing a 1g lateral pulse and observed torso-rollout. Parenteau (2006b) evaluated far-side occupant kinematics in a low-speed lateral sled in three different pulse conditions with three 50th percentile human volunteers (two male, one female) and Hybrid III 50th percentile male. The subjects were seated on the front passenger side of a small European car with no center console. The study provides lateral and vertical head and shoulder displacements as well as noting that one of the male volunteers slipped out of their shoulder belt during the impact event.

Research has suggested that better torso restraint and reduced lateral head displacement in far-side lateral crashes can be achieved by eliminating shoulder belt slack (Stolinski et al. 1998; Parenteau et al. 2006a; Douglas et al. 2011). Seat belt pre-tensioners are an advanced restraint system designed to remove shoulder belt slack prior to the occupant's forward torso excursion due to impact. They activate within the first milliseconds of an impact to ensure the seat belt is in an optimal position to provide restraint in the crash (Zellmer et al. 1998). Pre-tensioning systems tie the occupant to the vehicle's deceleration early during the crash, reducing the peak load by the occupant (Walz et al. 2004). These systems are intended to be most effective in the instance of frontal impacts (Zellmer et al. 1998; Walz et al. 2004; Forman et al. 2008). However, studies evaluating the effect of pre-tensioning in far-side impacts in adult volunteers have shown their ability to reduce lateral head displacements in far-side impacts by approximately 200 mm (Stolinski et al. 1999; Douglas et al. 2007).

We have previously evaluated the effect of electromechanical motorized seat belt retractor (EMSR) activation on the pediatric population in low-speed far-side lateral and oblique loading (Arbogast et al. 2012). The EMSR served to pre-tighten the seat belt very early in the impact similar to the action of a pre-tensioner. With a focus on the interaction between the torso and shoulder belt, we demonstrated that EMSR activation significantly reduces the forward and lateral displacement of the suprasternal notch, torso rollout angle (measured as the angle between the sternum and shoulder belt), and belt-sternal distance (distance between the suprasternal notch and shoulder belt in the x-y plane). Due to variations in neck mechanics with age (Arbogast et al. 2009; Seacrist et al. 2012), head and neck kinematics may differ from the observations made on the torso. As a result, the question remains as to the effect of EMSR activation on head kinematics for the pediatric population. Therefore,

we have undertaken this further analysis to evaluate the effect of EMSR activation on pediatric head and spine kinematics in far-side loading.

In order to optimally develop pre-tensioners or other countermeasures for far-side impacts, the kinematics of the occupant must be understood. Törnvall et al. (2005) comments on shoulder joint geometry and its interaction with the shoulder belt in limiting slippage out of the shoulder belt, and in turn head kinematics. Alterations in arm position influencing the shoulder joint and belt interaction should be evaluated.

Therefore, the objective of this study was to evaluate the effect of EMSR activation and arm position on head and spine kinematics of pediatric and young adult human volunteers in low-speed lateral and oblique loading conditions.

METHODS

This study protocol was reviewed and approved by the Institutional Review Boards at The Children's Hospital of Philadelphia, Philadelphia, PA, Rowan University, Glassboro, NJ and Drexel University, Philadelphia, PA.

Test Device

A pneumatically actuated – hydraulically controlled low speed crash sled that can be rotated and fixed in increments of 30°, shown in Figure 1, was designed to subject restrained human volunteers to a sub-injurious, low-speed lateral and oblique far-side crash pulse.

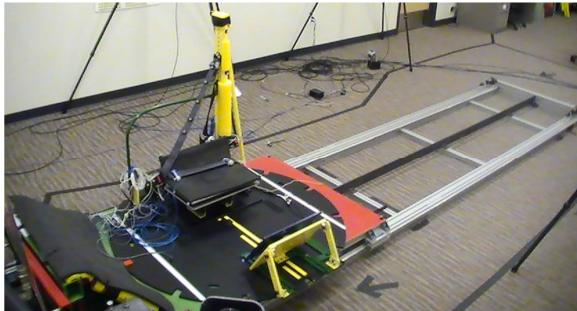


Figure 1. Low-speed volunteer crash sled

The sled is primarily comprised of three sub-assemblies, namely frame, actuator and seating buck. The frame was constructed of extruded aluminum tubing (MiniTec Framing Systems LLC, Victor, NY). The structural framework included a platform (for the actuator assembly) which was rigidly connected to two 6.1 m long parallel support rails with equally spaced cross members for rigidity. The actuator

assembly was comprised of a pneumatic actuator (McMaster-Carr, Robbinsville, NJ) (diameter – 4 inches, stroke length – 20 inches, operating pressure – 200 psi) connected to an opposing dual hydraulic piston-cylinder (Model TZ22, Vickers Cylinders, Eaton Corporation, Cleveland, OH) arrangement using a rigid frame. A 2-way high dynamics proportional throttle cartridge valve (Model LIQZOLE, Atos, Italy) was used in the custom-designed hydraulic circuit to control the displacement profile of the pneumatic actuator. When the pneumatic actuator was fired, it delivered the impact force to the seating buck. A pneumatic braking system gradually brought the sled to rest following the primary acceleration pulse. Two hydraulic dampers were mounted at the end of the rails to act as an emergency braking system, but these dampers were never engaged during any of the subject tests.

The seating buck assembly framework was also constructed using extruded aluminum tubing (MiniTec Framing Systems LLC, Victor, NY). It was comprised of a moving platform mounted on the two support rails by means of six low friction linear bearings. A custom-built impact fixture was mounted on the platform to transfer the force from the pneumatic actuator to the moving platform. A rigid low-back padded seat, an adjustable height shoulder belt anchor post (similar to a B-pillar in an automobile), lap belt anchors and an adjustable footrest (406 mm x 254 mm aluminum plate inclined at 55° from the platform) were mounted onto a disk bolted to the moving platform. The disk can be rotated and then fixed in 30° increments to test in a variety of impact directions. For the tests reported herein, the disk was fixed at 60° and 90° relative to longitudinal axis of the sled. The low-back seat was made of aluminum and consisted of a horizontal seat pan (495 mm x 305 mm) and a 127 mm high seat back reclined 18° from vertical. A 6.5 mm thick low-density polyurethane padding was adhered to the surface of the seat pan and seat back. The low-back seat was necessary to allow for the motion analysis markers along the spine to be visible to the cameras.

An automotive three-point belt system with an electromechanical motorized seat belt retractor (EMSR) integrated to the shoulder belt was used (Takata Corporation, Japan). The EMSR was powered by a 12V-20A battery and was activated 200 msec prior to the initiation of the crash pulse. It achieved a pre-tensioning load of approximately 300N. The rise time to peak load was 100 msec. The restraint system was designed such that the EMSR could be either active or inactive and its firing control was integrated into the sled pulse triggering system.

Safe Volunteer Crash Pulse

An amusement park bumper car ride was studied to provide a benchmark of a crash-like situation commonly and safely used by children for recreation and enjoyment. Safe limits on the volunteer crash pulse were defined from measuring a lateral impact to a bumper car by another bumper car in an amusement park (Funtown Pier, Seaside Park, NJ). An accelerometer was secured to the rigid cross-member of the steering assembly of a bumper car. The average maximum acceleration obtained when the bumper car was impacted laterally was 2.54 g. This was defined as the envelope of safety for the human volunteers. For the subject trials, the acceleration was reduced by 20% to produce a maximum pulse of 2.0 g. Several safety checks ensured that the system delivered the appropriate pulse (Arbogast et al. 2009).

An exemplar sled pulse is displayed in Figure 2. The activation of the synchronous trigger was followed by a time delay before the movement of the sled (event). The time delay (approximately 203 msec) was attributed to the response lag associated with the sled hydraulic system. Event onset (vertical line in Figure 4) was defined as the time at which the sled acceleration reached 5% of its peak value and for all time series analyses was considered time zero. For the EMSR tests, activation occurred synchronously with the trigger.

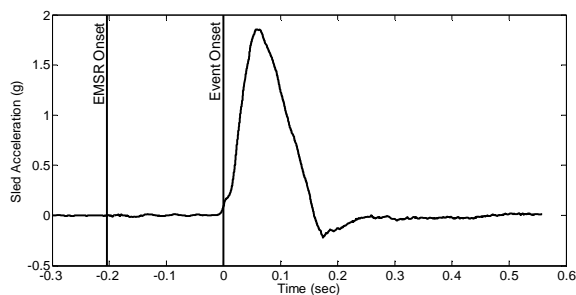


Figure 2. Exemplar Crash Pulse. Event onset is defined as the time at which the sled acceleration reached 5% of its peak value and was considered time zero. The EMSR (and sled) was fired approximately 200 ms prior to event onset.

Human Subjects

Specific inclusion criteria were male subjects aged between 9-14 years and 18-30 years whose height, weight and BMI were within 5th and 95th percentile for the subject's age (based upon CDC growth charts for children and CDC NHANES data for subjects 18+ years). Subjects with existing neurologic, orthopedic, genetic, or neuromuscular conditions, any

previous injury or abnormal pathology relating to the head, neck or spine were excluded from the study. Subjects were recruited from flyers placed in the community and throughout CHOP and Rowan sites. Prior to the testing dates, telephone interviews were conducted with the adult subjects and parent /guardian of child subjects to confirm eligibility.

Upon arrival at the test site, the study was explained in detail to the subject including a demonstration of how the volunteer sled functions by firing the sled without an occupant. The adult subjects were given a self-consent letter and the parent / guardian of the child subjects were given a parental consent letter with a child subject assent. After the subjects had been consented, height and weight were measured to verify that their height, weight and body mass index (BMI) were consistent with the inclusion criteria. The subjects experienced one sled run with no subject instrumentation to ensure they were comfortable with the test protocol.

The subjects were asked to remove their shirt(s) and the following anthropometric measurements were recorded:

- Head width, depth, and girth measured at the glabella
- Neck width, depth, and girth measured at the laryngeal prominence, and length defined as opisthocranium to C7
- Shoulder width defined as acromion to acromion width
- Chest depth and width measured at the xiphoid process
- Sternum height measured from suprasternal notch to xiphoid process
- Waist girth measured at the umbilicus
- Hip width measured at the bilateral iliac crests
- Seated height
- Buttock to popliteal length while seated
- Knee to foot length while seated

Instrumentation

Spherical reflective markers were placed on the head, neck, torso, upper and lower extremities, shoulder belt and various locations on the seating buck and tracked using a 3D motion analysis system (Model Eagle 4, Motion Analysis Corporation, Santa Rosa, CA). The accuracy of this system was verified by a static and dynamic calibration procedure that resolved a 500mm calibration distance to 0.1 mm. The photoreflexive targets were attached to the following anatomical landmarks through external palpation of the desired skeletal locations:

- Head
 - On headpiece – head top, left, right, front, and opisthocranium
 - External auditory meatus (bilateral)
 - Nasion
- Torso
 - Suprasternal notch
 - Mid-clavicular (right)
 - Xiphoid process
 - Pectoralis (right)
 - Nipple (right)
 - Lateral most aspect of neck (right)
 - Acromion (bilateral)
- Spine
 - C4; T1; T4; T8; and T12
- Extremities
 - Humeral epicondyle (bilateral)
 - Ulnar styloid process (bilateral)
 - Iliac crest (bilateral)
 - Femoral epicondyle (bilateral)
 - Lateral malleolus (bilateral)

Three angular rate sensors – ARS (ARS-1500, DTS Inc, Seal Beach, CA) were mounted orthogonal to each other via a custom fixture to a rigid head piece to measure the head rotational velocity. The custom fixture secured on the head, additionally held three orthogonal piezoresistive accelerometers (Model 7264B-500, Endevco, San Juan, CA) to measure head acceleration. A piezoresistive accelerometer (Model 7264-200, Endevco, San Juan, CA) was mounted to the moving platform frame to record the acceleration of the seating buck. Lightweight belt webbing load cells (Model 6200FL-41-30, Denton ATD Inc, Rochester Hills, MI) were attached 13 cm from the D-ring location on the shoulder belt between the subject and the D-ring and on the right and left locations on the lap belt. A single six-axis load cell was placed under the seat pan (Model IF-217, FTSS, Plymouth, MI) and one under the footrest (Model IF-234, FTSS, Plymouth, MI), to measure the reaction forces exerted by the subjects. A high-speed video camera (MotionXtra HGTH, Redlake, San Diego, CA) oriented perpendicular to the frontal plane of the occupant recorded the qualitative relative movement of the head, torso and the shoulder belt at a rate of 1,000 frames per second (fps). In addition, two standard video camcorders were used to capture the kinematics of the occupant at 30 fps.

Subject Positioning and Test Matrix

After the instrumentation setup was completed, the subjects were seated and restrained in the volunteer sled as shown in Figure 3. The initial position of the torso and knee angles was set to 110° by adjusting the fore-aft position of the footrest. The initial torso

angle was defined as the angle made by the line joining the right iliac crest and right acromion markers and the horizontal. The initial knee angle was defined as the angle between the line joining the right iliac crest and right femoral epicondyle markers and the line joining the right femoral epicondyle and right lateral malleolus markers. The lap belt anchor locations were fixed throughout the test series and the lap belt buckle angle (defined as the angle the lap belt buckle makes with the horizontal) was set at 55° at initial position for all the subjects. The height of the shoulder belt anchor was adjusted to provide similar fit across subjects; specifically, the shoulder belt angle at the D-Ring (defined as the angle the shoulder belt makes with the horizontal) was set at 55° at initial position for all the subjects. Once positioned, the shoulder belt was snugged to fit optimally for the subject's size. The subjects wore a tightly fitted headpiece with six head markers (top, front, left, right, opisthocranium right and left) and a triaxial accelerometer and angular rate sensor block attached.

Each subject was randomly assigned to the 60° or 90° direction and was tested only in their assigned direction. Each subject was exposed to 4 unique test conditions in random order - arms up with EMSR on, arms down with EMSR on, arms up with EMSR off, and arms down with EMSR off (Table 1). Each test condition was repeated twice. In the arms up condition, the subject was instructed to place their hands on their knees. This raised the upper extremity and created an anatomic pocket at the clavicle in which the shoulder belt could rest. In the arms down condition, the subject was instructed to place their hands low on their hips, thereby removing the anatomic pocket at the clavicle. The order of the tests was chosen at random. Subjects were informed that they could withdraw from the study at any time. Before each test, the occupant was encouraged to relax their muscles and allow the restraints to support their weight during the acceleration event. Subjects received an auditory countdown in each test prior to the firing of the actuator. All the tests were conducted with a rest period of approximately 5 minutes between subsequent tests.



Figure 3. Subject seated in low-speed volunteer sled – “arms up” position.

Table 1.

Test matrix for each subject. Subjects were tested in only one direction (oblique or lateral) and trial order was randomized.

	EMSR activation	
Arm position	On	Off
Arms-Up (hands on knees)	2 Trials	2 Trials
Arms-Down (hands on thighs)	2 Trials	2 Trials

Data Acquisition/Processing

The Motion Analysis data were acquired at 100 Hz and analyzed using Cortex 2.5 software (Motion Analysis Corporation, Santa Rosa, CA). The sled acceleration, head angular rate, head acceleration and seat belt, seat pan and foot rest loads were sampled at 10,000 Hz using a T-DAS data acquisition system (Model T-DAS Pro, DTS Inc, Seal Beach, CA) with a built-in anti-aliasing filter (4,300 Hz) and filtered at SAE channel frequency class (CFC) 60, as described in the SAE J211 standards. The hydraulic controller, motion analysis, T-DAS systems and EMSR (where applicable) were triggered synchronously using a custom made circuit.

Data Analysis

The time series motion analysis and T-DAS data were imported into MATLAB (Mathworks, Inc., Natick, MA) for data analysis using a custom program. The parameters of interest are:

- 1) Maximum forward (X) and lateral (Y) displacement of the Head Top marker
- 2) Maximum forward (X) and lateral (Y) displacement of the C4, T1, and T4 markers.

Displacement was measured by quantifying the motion of the head top and spine markers in the forward (x) and lateral (y) direction, relative to initial position ($t = \text{event onset}$). The origin of the local coordinate system was defined as the marker at the right rear of the seat pan.

Using separate models for 60 and 90 degrees, data were statistically analyzed using repeated measures analysis with a linear mixed model, observing the effect of EMSR (on/off) and Arm Position (up/down) as covariates for each outcome. A Compound Symmetry covariance model was used to control the correlation between the two Arms/EMSR conditions within each subject. For each outcome, we first examined a full model which included all of the covariates and interactions. Then, each model was reduced to a final model by first taking out non-significant interaction effects and then main effects, one by one, until all covariates were statistically significant at the 5% level. A statistical model was created separately for the following outcomes:

- Head Top displacement
 - Maximum forward displacement of the head top
 - Maximum lateral displacement of the head top
- C4 displacement
 - Maximum forward displacement of the C4
 - Maximum lateral displacement of the C4
- T1 displacement
 - Maximum forward displacement of the T1
 - Maximum lateral displacement of the T1
- T4 displacement
 - Maximum forward displacement of the T4
 - Maximum lateral displacement of the T4

RESULTS

Thirty male human volunteers were tested: fifteen subjects at each impact angle (60° and 90°), with five subjects per age group (9-11 years, 12-14 years, 18-30 years). Key anthropometric measures are listed in Table 2.

The maximum acceleration for the 60° trials was 1.88 g (rise time of 52.7 msec, pulse duration: 147 msec) and for the 90° trials it was 1.91 g (rise time of 54.3 msec, pulse duration: 146.7 msec).

Figure 4 depicts exemplar head top trajectories of a pediatric (13 y/o) subject in the arms up condition subjected to a lateral impact.

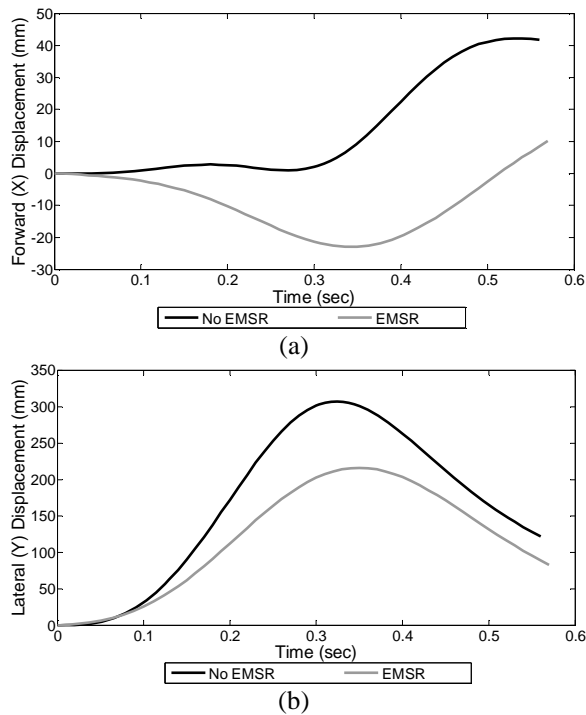


Figure 4. Exemplar (a) forward and (b) lateral displacement over time of the head top marker with and without EMSR activation in the arms up position for one pediatric subject at 90°. Displacement is shown relative to initial position.

Forward Displacement

Maximum forward displacement of the head top and spine markers for each test condition and both impact angles are seen in Figure 5. Figure 6 shows maximum forward displacement of the head top marker across age as a continuous variable, stratified by EMSR activation and arm position.

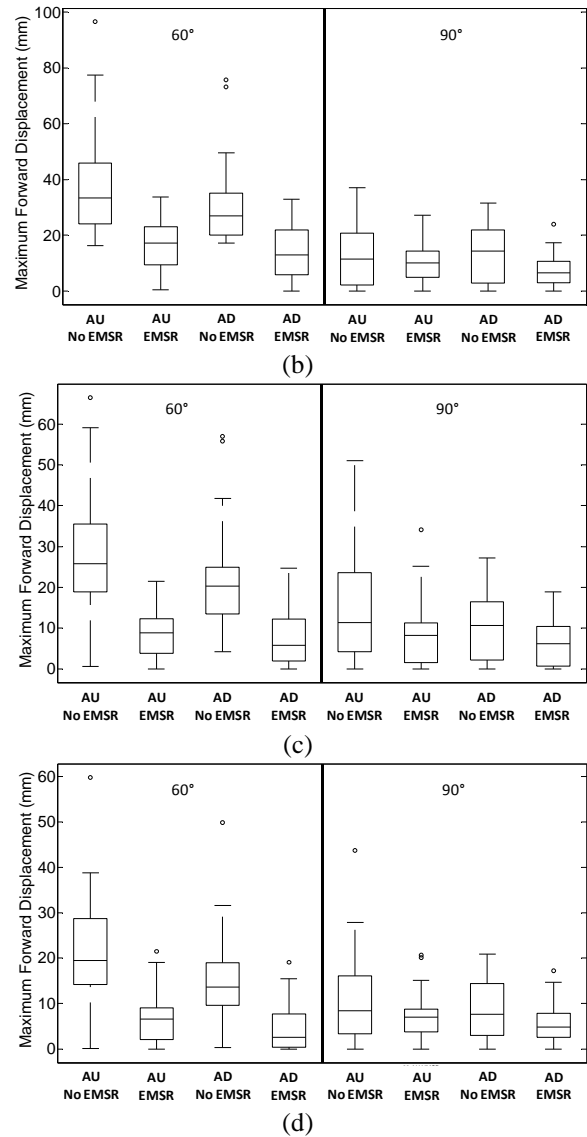
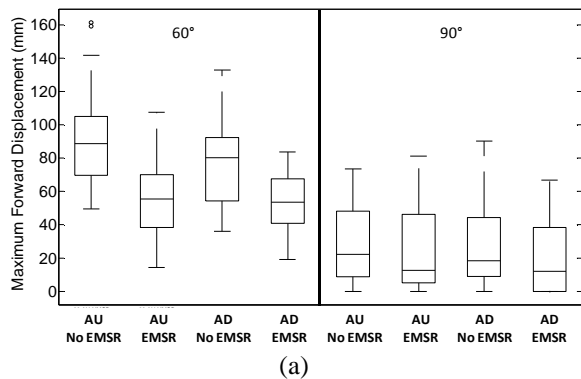


Figure 5. Maximum Forward Displacement of (a) Head Top, (b) C4, (c) T1, and (d) T4 markers, where AU is arms up and AD is arms down. All subjects, all trials are included.

Table 2.
Key anthropometric parameters for subjects.

Impact Angle	Subject #	Age (yrs)	Height (cm)	Height %ile	Mass (kg)	Mass %ile	BMI (kg/m³)	BMI %ile
60°	1	9.62	144.0	85	48.0	95	23.1	25
	2	10.30	134.5	22	27.4	14	15.2	17
	3	10.54	136.0	19	28.1	11	15.2	21
	4	11.58	149.0	62	43.3	71	19.5	81
	5	11.69	150.5	66	37.6	42	16.6	35
	9-11 Avg.	10.74	142.8	50.8	36.9	46.6	17.9	35.8
	6	12.88	158.0	61	54.1	81	21.7	85
	7	14.01	159.0	25	64.5	87	25.5	95
	8	14.07	172.0	84	60.7	80	20.5	73
	9	14.19	177.5	93	66.5	88	21.1	77
	10	14.31	164.0	40	54.2	56	20.2	66
	12-14 Avg.	13.89	166.1	60.6	60.0	78.4	21.8	79.2
	11	20.17	182.5	75	95.7	85	28.7	85
	12	22.30	172.5	24	74.9	50	25.2	65
	13	22.75	176.0	48	74.8	50	24.2	53
14	23.16	181.0	74	90.5	80	27.6	76	
15	23.34	185.5	80	95.8	80	27.8	74	
Young Adult Avg.	22.34	179.5	60.2	86.4	69.0	26.7	70.6	
90°	16	9.29	145.0	93	34.9	81	16.6	58
	17	10.30	139.0	46	33.9	58	17.5	71
	18	11.13	141.5	32	31.6	21	15.8	30
	19	11.20	153.5	89	36.9	50	15.6	23
	20	11.97	152.0	65	36.3	29	15.7	21
	9-11 Avg.	10.78	146.2	65.0	34.7	47.8	16.3	40.6
	21	12.96	149.0	17	50.5	70	22.7	91
	22	13.34	160.0	54	43.7	32	17.1	22
	23	13.53	148.0	6	36.7	6	16.8	19
	24	13.69	160.0	42	49.9	52	19.5	58
	25	14.99	159.0	25	47.2	33	18.7	48
	12-14 Avg.	13.70	155.2	28.8	45.6	38.6	18.9	47.6
	26	19.70	182.0	75	75.6	51	22.8	45
27	20.55	184.0	80	87.7	77	25.9	68	
28	20.86	184.0	80	83.2	76	24.6	57	

	29	21.69	184.0	80	83.5	76	24.7	58
	30	21.90	174.0	28	76.7	50	25.3	44
	Young Adult Avg.	20.94	181.6	68.6	81.3	66.0	24.7	54.4

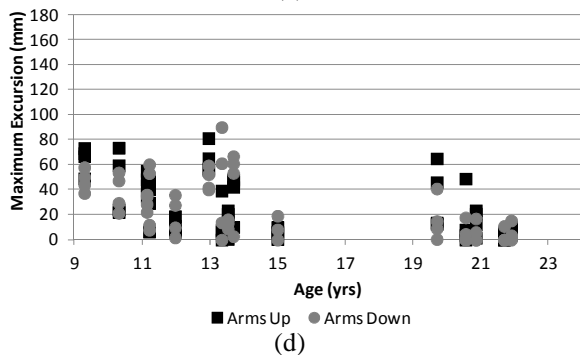
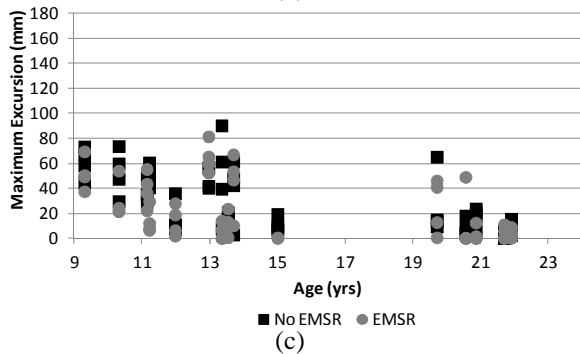
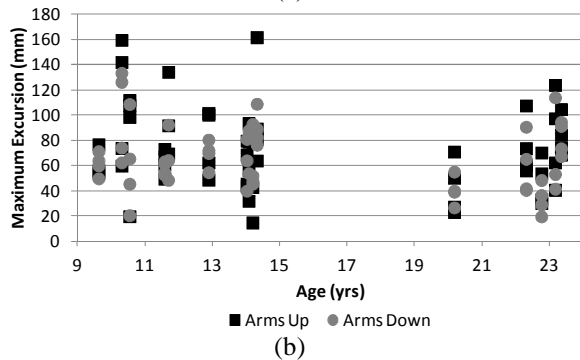
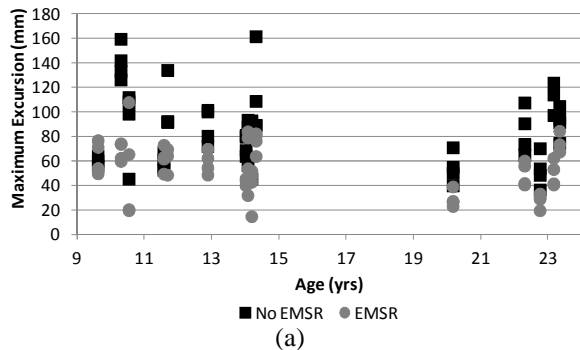


Figure 6. Maximum Forward Head Top Displacement across age as a continuous variable (a) 60° impact, stratified by EMSR activation; (b) 60°

impact, stratified by arm position; (c) 90° impact, stratified by EMSR activation; (d) 90° impact, stratified by arm position.

Average maximum forward displacement and standard deviation of each marker are provided in Table 3. Statistical findings of the head top and spine forward displacements are summarized in Table 4.

Figure 5a, as well as the head top mean and standard deviation values in Table 3, highlights the lesser magnitudes of the forward head excursions in the 90° trials compared to the 60° trials. EMSR activation significantly reduced head and spine forward displacements in the oblique impacts, while only spine forward displacements were significantly decreased in the lateral impacts. In both the 60° and 90° trials, arm position did not significantly influence head top forward displacement. However, C4 and T4 forward excursions were significantly increased in the arms up position relative to arms down at 60°. At both impact angles there was a marginally significant increase of T1 forward excursions ($p = 0.051$ at 60° and $p = 0.052$ at 90°) in the arms up position. Arm position did not have a significant effect on maximum forward displacement in the 90° impacts.

Table 3. Maximum Forward Displacement (mm)

	Mean (St. Dev.)	EMSR Activation		Arm Position	
		On	Off	Up	Down
60°	Head Top	54.1 (19.9)	84.6 (29.1)	72.9 (32.3)	65.5 (25.2)
	C4	15.4 (9.0)	34.6 (17.3)	27.4 (18.1)	22.2 (14.9)
	T1	8.5 (6.8)	25.6 (14.7)	19.1 (15.5)	14.8 (12.6)
	T4	5.8 (5.6)	18.7 (11.4)	14.1 (11.9)	10.3 (9.9)
90°	Head Top	22.3 (23.0)	29.4 (23.4)	27.4 (24.0)	24.4 (22.8)
	C4	8.5 (6.9)	13.2 (10.7)	11.2 (9.7)	10.7 (9.1)
	T1	7.5 (7.2)	12.8 (11.8)	11.9 (12.2)	8.4 (7.3)
	T4	6.3 (5.0)	9.4 (8.3)	9.0 (7.9)	6.7 (5.7)

Table 4.
Maximum Forward Displacement Summary Statistics

	60°		90°	
	EMSR (ref: off)	Arm Position (ref: down)	EMSR (ref: off)	Arm Position (ref: down)
Head Top	↓***	--	--	--
C4	↓***	↑*	↓*	--
T1	↓***	--	↓**	--
T4	↓***	↑*	↓*	--

The arrow indicates the direction of the relationship.
*p < 0.05, **p < 0.01, ***p < 0.001

Lateral Displacement

Maximum lateral displacement for these markers is shown in Figure 7. Figure 8 shows maximum lateral displacement of the head top marker across age as a continuous variable, stratified by EMSR activation and arm position.

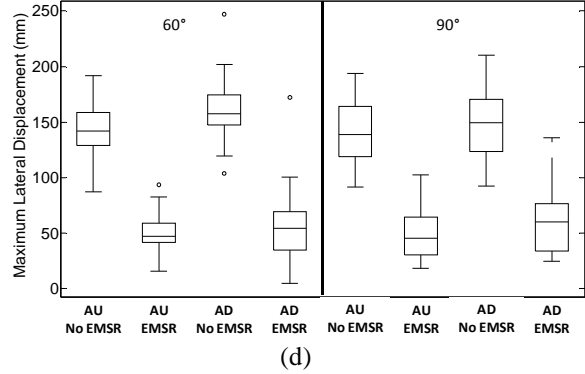
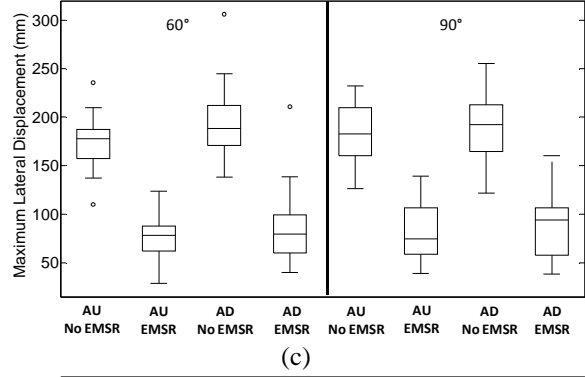
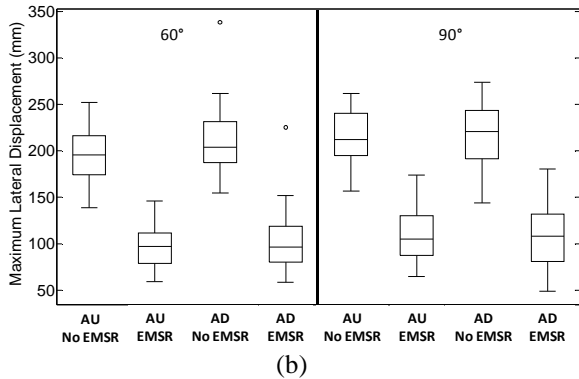
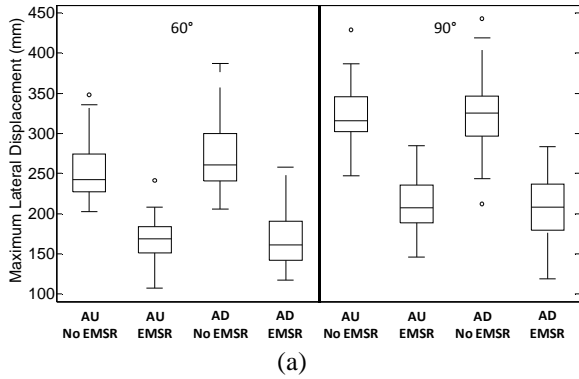
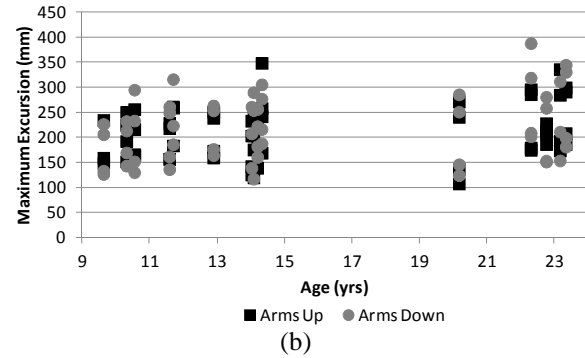
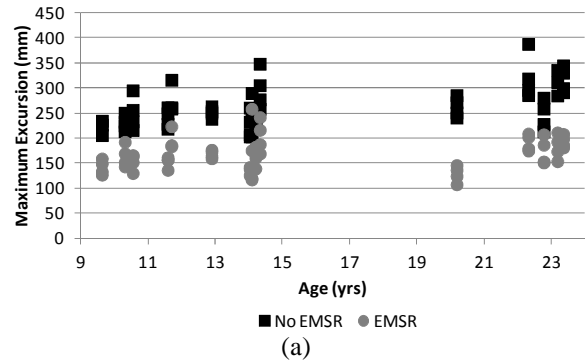


Figure 7. Maximum Lateral Displacement of (a) Head Top, (b) C4, (c) T1, and (d) T4 markers, where AU is arms up and AD is arms down. All subjects, all trials are included.



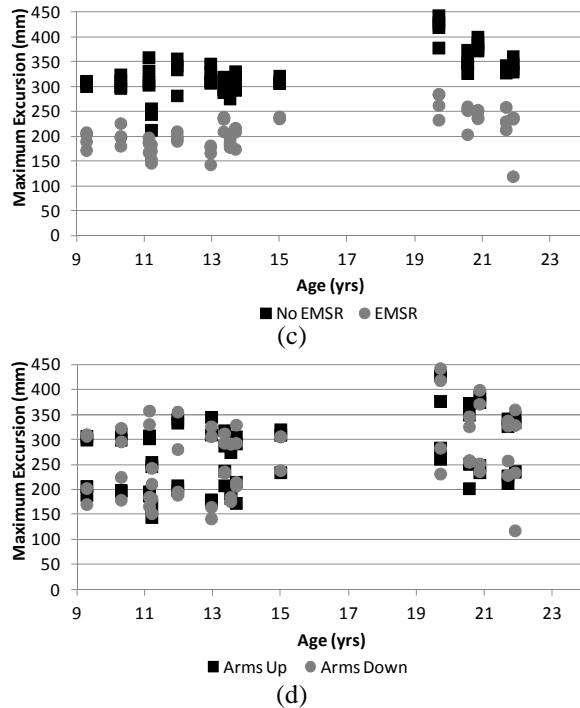


Figure 8. Maximum Lateral Displacement of Head Top across age as a continuous variable (a) 60° impact, stratified by EMSR; (b) 60° impact, stratified by arm position; (c) 90° impact, stratified by EMSR activation; and (d) 90° impact, stratified by arm position.

Table 5. Maximum Lateral Displacement (mm)

	Mean (St. Dev.)	EMSR Activation		Arm Position	
		On	Off	Up	Down
60°	Head Top	167.95 (31.25)	261.63 (40.95)	210.03 (53.86)	218.80 (64.69)
	C4	100.06 (28.96)	203.49 (33.32)	144.77 (54.41)	156.90 (65.98)
	T1	80.26 (29.60)	183.52 (31.75)	124.46 (54.65)	138.55 (65.05)
	T4	52.99 (26.73)	151.03 (26.28)	95.85 (50.86)	107.42 (60.42)
90°	Head Top	209.17 (35.40)	324.45 (42.47)	268.32 (67.00)	267.26 (73.03)
	C4	108.93 (29.86)	216.81 (30.97)	164.78 (60.71)	164.44 (64.07)
	T1	82.75 (27.91)	189.05 (31.35)	133.70 (60.21)	139.91 (62.18)
	T4	54.41 (24.47)	145.75 (29.63)	97.34 (53.14)	104.36 (53.62)

Table 6. Maximum Lateral Displacement Summary Statistics

	60°		90°	
	EMSR (ref: off)	Arm Position (ref: down)	EMSR (ref: off)	Arm Position (ref: down)
Head Top	↓***	--	↓***	--
C4	↓***	↓*	↓***	--
T1	↓***	↓***	↓***	--
T4	↓***	↓**	↓***	--

The arrow indicates the direction of the relationship. *p < 0.05, **p < 0.01, ***p < 0.001

Maximum lateral displacement mean and standard deviation of each marker are provided in Table 5. Summarized statistical findings of the head top and spine lateral displacements are in Table 6. Maximum lateral displacement of the head top and spine markers were significantly reduced by EMSR activation in the 60° and 90° impacts. The arms up position was significantly less than arms down for the spine maximum lateral displacements in the oblique impacts. There was no significant effect of arm position in the lateral impacts.

DISCUSSION

The objective of this study was to evaluate the effect of pre-tensioning in form of EMSR activation and arm position on the forward and lateral displacement of the head and spine in far-side low-speed lateral and oblique collisions. These data represent the first collected on pediatric male volunteers in the far-side loading condition.

EMSR activation significantly reduced lateral head and spine displacements at both impact angles. Far-side studies utilizing computational models, PMHS, ATDs, and adult volunteers similarly showed reduced lateral head displacements as a result of pre-tensioning (Stolinski et al. 1999; Parenteau 2006b; Douglas et al. 2007; Pintar et al. 2007; Douglas et al. 2011). Pintar et al. (2007) noted only slight reductions (50 mm) in maximum lateral head excursions with pre-tensioning and moving the D-ring rearward for adult PMHS subjected to far-side lateral loading (Delta V: 30 km/h). The coupling of pre-tensioning and rearward D-ring position, along with the initial position of the PMHS arms outstretched could minimize the effect of pre-tensioning on the PMHS lateral head excursions.

However, pre-tensioning reduced lateral head displacement of 50th percentile Hybrid III and US-SID by almost 200 mm in car-to-car lateral impacts (50 km/h) (Stolinski et al. 1999). The effect of pre-tensioning on adult anthropometry is well established in previous literature and the effect of EMSR activation on adult subjects in the current study confirms those observations (116 mm and 127 mm reduction for oblique and lateral impacts respectively). The study herein extended previous literature and also evaluated pediatric subjects. Figures 8a and 8c demonstrate the effectiveness of EMSR activation in reducing pediatric lateral head displacement. EMSR activation reduced pediatric lateral head displacement by 83 mm in 60° impacts and 110 mm in 90° impacts.

The benefits of EMSR activation were also seen in the spine. C4, T1, and T4 lateral displacement significantly decreased with EMSR activation. These findings are congruent with the significant reduction in suprasternal notch lateral displacement and torso-rollout angle reported by Arbogast et al. (2012) of the same loading environment. Quasi-static lateral (1 g) impact tests with male adult volunteers also showed a decrease in T1 lateral displacement of approximately 25 mm with a pre-tensioning load of 225 N (Douglas et al. 2007). In the current study, EMSR activation with a pre-tensioning load of approximately 300 N reduced T1 lateral displacement by 106 mm in the 90° impacts.

Pre-tensioners are primarily designed to limit forward excursion in frontal impacts (Zellmer 1998; Walz 2004). These data confirm this effect in that forward excursions of the head top and spine were significantly reduced with EMSR activation in the 60° impacts, and for the spine in the 90° impacts.

Interestingly, EMSR activation not only reduced the forward and lateral displacement magnitude but also the variability across age at both impact angles (Figures 6a, 6c, 8a, and 8c). Pre-tensioning is an advanced restraint system primarily implemented as a safety countermeasure for front-seat occupants. Since rear-seat occupants also include child passengers, the range of occupant sizes in the rear seat present a challenge for the safety industry to account for with advanced restraint systems. The results of this study suggest that EMSR activation would be effective in reducing occupant motion for child and adult passengers with varying anthropometry.

Raising the arms to create a pocket for the shoulder belt significantly reduced lateral spine excursions relative to the arms down position in the 60° impacts.

Törnvall et al. (2005) suggests that altering the shoulder joint geometry where it contacts the shoulder belt could influence the kinematics of the occupant. We explored this hypothesis by implementing two arm positions as part of the experimental design. In the arms up position, placing the hands on the knees raises the upper extremity and consequently the acromial end of the clavicle, creating an anatomic pocket that can engage the shoulder belt. The arms down position provides a smooth contour along the clavicle that facilitates the shoulder belt sliding off. The oblique impacts provide a principal direction of force to the occupant that result in better engagement of the shoulder belt with the clavicle and thereby restricting the lateral motion of the occupant's spine, especially in the arms up position (Pintar et al. 2007; Douglas et al. 2011). In contrast, raising the arms significantly increased forward spine displacement in the 60° trials. As the shoulder belt catches on the anatomic pocket created by elevating the arms and the occupant responds to the oblique principal direction of force, the torso may respond to the shoulder belt load by flexing forward in contrast to when the shoulder belt slides off the shoulder in the arms down position and no load is placed on the clavicle.

There were several limitations to this study. The acceleration pulse for the study must be sub-injurious for human volunteer subjects. While the maximum acceleration reported herein is not of the same magnitude as real-world lateral and oblique crashes, the low-speed crash environment provides a fundamental understanding of occupant head and spine kinematics at these impact angles. Secondly, the experimental test matrix implemented in this study does not comprehensively explore all factors influencing head and spine kinematics under lateral and oblique loading in a full factorial design for a single subject. Since pediatric volunteers participated in the study, the subject's ability to endure the lengthy test protocol had to be taken into consideration and therefore the factors of greatest interest were incorporated. Additionally, the head and spine kinematics were measured using a 'state of the art' 3D motion capture system utilizing markers affixed to the skin. There are two sources of error associated with this methodology. First the motion capture system has intrinsic error. This error, estimated by measuring the change in distance over time between two markers on the cart, averaged 0.3%. Second, some error exists in assuming the skin markers exactly match the movement of the skeletal structures they represent. The magnitude of this error can, in part, be assessed by examining the change in distance over time between markers affixed to two

points on the same skeletal body. We have previously quantified this to be less than 2% for this testing environment (Arbogast et al. 2009). Also, gender differences in neck flexibility have been observed in the passive cervical range of motion in male and female children and adults (Seacrist et al. 2012). Since the results reported in the current study are based on male-subjects' kinematic responses, they may not be generalized to the entire population. Lastly, a single electromechanical motorized seat belt retractor was implemented in this experiment which provided a constant pre-tensioning load that did not vary with mass. Future work should be conducted to evaluate the effect of pre-tensioning on head and spine kinematics by utilizing such technology with varying load capabilities and adjustments with subject mass.

CONCLUSIONS

The objective of this study was to evaluate the effect of pre-tensioning in the form of EMSR activation and arm position on pediatric and young adult male volunteers subjected to low-speed far-side oblique and lateral loading. This study provided the first pediatric volunteer data set for head and spine kinematics in far-side loading conditions. EMSR activation significantly reduced head and spine kinematics at both impact angles, for both pediatric and young adult subjects. EMSR activation also reduced variability in kinematics across age. The arms up position significantly decreased spine lateral excursions in the 60° impacts. These findings can be influential in vehicle safety design for rear seat occupants through the validation of restrained ATD and computational modeling studies in far-side loading conditions.

ACKNOWLEDGEMENTS

The authors would like to thank all the human volunteers who participated in this study for their patience and willingness to take part in this research, Robert Sterner, PhD and the Department of Health and Exercise Science at Rowan University for the use of the motion capture laboratory, Charles Linderman and Kyle Fitzpatrick from the Department of Mechanical Engineering at Rowan University for sled modifications, Steve Moss from Diversified Technical Systems for contributions to the instrumentation, Lawrence Chickola from Six Flags Theme Parks for access to the bumper car system, Lucy Robinson, PhD from the Department of Epidemiology and Biostatistics at Drexel University for statistical analysis guidance, and Caitlin Locey, Mari Allison, Aditya Belwadi, Megha Kamath and

Kelsey Lewis for assistance in data collection and processing. The authors would like to acknowledge Takata Corporation, Japan for their collaboration and financial support for this study. The results presented in this report are the interpretation solely of the author(s) and are not necessarily the views of Takata Corporation.

REFERENCES

- [1] Arbogast KB, Balasubramanian S, Seacrist T, Maltese MR, Garcia-Espana JF, Hopely T, Constans E, Lopez-Valdes FJ, Kent RW, Tanji H, Higuchi K. Comparison of Kinematic Responses of the Head and Spine for Children and Adults in Low-Speed Frontal Sled Tests. *Stapp Car Crash Journal* 2009. 53: 329-372.
- [2] Arbogast KB, Mathews EA, Seacrist T, Maltese MR, Hammond R, Kent RW, Tanji H, St. Lawrence S, Higuchi K, Balasubramanian S. The Effect of Pretensioning and Age on Torso Rollout in Restrained Human Volunteers in Far-Side Lateral and Oblique Loading. *Stapp Car Crash Journal*. 2012. Vol 56.
- [3] Bidez MW, Hauschild HW, Mergl KM, Syson S. Small Occupant Dynamics in the Rear Seat: Influence of Impact Angle and Belt Restraint Design. *SAE International* 2005. Paper No. 2005-01-1708.
- [4] Centers for Disease Control and Prevention. 2000. "Growth Charts – 2000 CDC Growth Charts." <http://www.cdc.gov/GrowthCharts/>
- [5] Digges K and D Dalmotas. Injuries to Restrained Occupants in Far-Side Crashes. Conference Proceedings of the 17th International Technical Conference on the Enhanced Safety of Vehicles 2001.
- [6] Digges K, Gabler H, Mohan P, Alonso B. Characteristics of the Injury Environment in Far-Side Crashes. Annual Proceedings of the Association for Advancement of Automotive Medicine 2005.
- [7] Douglas C, Fildes B, Gibson T. Modeling Occupants in Far-Side Impacts, *Traffic Injury Prevention* 2011. 12:5, 508-517.
- [8] Douglas CA, Fildes BN, Gibson TJ, Bostrom O, Pintar FA. Factors influencing occupant-to-seat belt interaction in far side crashes. *Annual*

- Proceedings, Association for the Advancement of Automotive Medicine 2007. 51: 319–339.
- [9] Forman, J, Michaelson, J, Kent, R, Kuppa, S, Bostrom, O. Occupant Restraint in the Rear Seat: ATD Responses to Standard and Pretensioning, Force-Limiting Belt Restraints. *Annu. Proc. Assoc. Adv. Automot. Med.* 2008. 52: 141-154.
- [10] Gabler HC, Digges K, Fildes BN, Sparke L. Side Impact Injury Risk for Belted Far Side Passenger Vehicle Occupants. *SAE World Congress 2005.* 2005-01-0287.
- [11] Horsch J, Schneider D, Kroell C. Response of belt restrained subjects in simulated lateral impact. In: *Proceedings of 23rd Stapp Car Crash Conference 1979.* Warrendale, Pa.
- [12] Horsch J. Occupant Dynamics as a Function of Impact Angle and Belt Restraint. *Proceedings of the 24th Stapp Car Crash Conference 1980.* SAE Paper 801310, pp. 417–438.
- [13] Mackay G, Hill J, Parkin S, Munns J. Restrained Occupants on the Nonstruck Side in Lateral Collisions. *Accident Analysis and Prevention* 1993. Vol. 25, No. 2, pp. 147-152.
- [14] Maltese MR, Chen I, Arbogast KB. Effect of Increased Rear Row Occupancy on Injury to Seat Belt Restrained Children in Side Impact Crashes. *Annual Proceedings of the Association for the Advancement of Automotive Medicine* 2005.
- [15] NHANES, 1994. “Center for Disease Control and Prevention Anthropometric reference data (1988-1994).” http://www.cdc.gov/nchs/about/major/nhanes/anthropometric_measures.htm
- [16] Parenteau C. A Comparison of Volunteers and Dummy Upper Torso Kinematics with and Without Shoulder Belt Slack in a Low Speed Side/Pre-Roll Environment. *Traffic Injury Prevention* 2006a. 7(2): 155-163.
- [17] Parenteau C. Far-Side Occupant Kinematics in Low Speed Lateral Sled. *Traffic Injury Prevention* 2006b. 7(2): 164-170.
- [18] Pintar F, Yoganandan N, Stemper B, Bostrom O, Rouhana SW, Smith S, Sparke L, Fildes BN, Digges KH. WorldSID Assessment of Far Side Impact Countermeasures. *Proceedings of 50th Stapp Car Crash Conference* 2006.
- [19] Ryb GE, Dischinger PC, Braver ER, Burch CA, Ho SM, Kufera JA. Expected Differences and Unexpected Commonalities in Mortality, Injury Severity, and Injury Patterns Between Near Versus Far Occupants of Side Impact Crashes. *Journal of Trauma* 2009. 66(2): 499-503.
- [20] Seacrist T, Saffioti J, Balasubramanian S, Kadlowec J, Sterner R, García-España JF, Arbogast KB, Maltese MR. Passive cervical spine flexion: the effect of age and gender. *Clin Biomech* 2012. (Bristol, Avon). 27(4):326-33.
- [21] Stolinski R, Grzebieta R, Fildes B. Side Impact Protection - Occupants in the Far-Side Seat, *International Journal of Crashworthiness* 1998. Vol.3 No. 2, pp 93-122.
- [22] Stolinski R, Grzebieta RH, Fildes BN, Judd R, Wawrzynczak J, Gray I, McGrath P, Case M. Response of Far side Occupants in Car-To-Car Impacts With Standard and Modified Restraint Systems Using Hybrid III and US- SID. *SAE* 1999. Paper 1999-01-1321.
- [23] Törnqvist FV, Svensson MY, Davidsson J, Flogård A, Kallieris D, Håland Y. Frontal Impact Dummy Kinematics in Oblique Frontal Collisions: Evaluation Against Post Mortem Human Subject Test Data. *Traffic Injury Prevention* 2005. 6(4): 340-350.
- [24] Viano DC and CS Parenteau. Severe Injury to Near- and Far-Seated Occupants in Side Impacts by Crash Severity and Belt Use, *Traffic Injury Prevention* 2010. 11:1, 69-78.
- [25] Walz M. NCAP test improvements with pretensioners and load limiters. *Traffic Inj Prev.* 2004. 5(1):18–25.
- [26] Zellmer H, Luhrs S, and Bruggermann K. Optimized restraint systems for rear seat passengers. *Proceedings of the 16th International Conference on the Enhanced Safety of Vehicles* 1998.